Nonideal optical response of liquid crystal variable retarders and its impact on their performance as polarization modulators

Cite as: J. Vac. Sci. Technol. B **38**, 014009 (2020); https://doi.org/10.1116/1.5122749
Submitted: 31 July 2019 . Accepted: 02 December 2019 . Published Online: 20 December 2019

Pilar García Parejo, Antonio Campos-Jara, Enric García-Caurel, Oriol Arteaga, and Alberto Álvarez-Herrero

JVST B
Journal of Vacuum Science & Technology B

ARTICLE

avs.scitation.org/journal/jvb

Nonideal optical response of liquid crystal variable retarders and its impact on their performance as polarization modulators

Cite as: J. Vac. Sci. Technol. B 38, 014009 (2020); doi: 10.1116/1.5122749
Submitted: 31 July 2019 · Accepted: 2 December 2019 ·
Published Online: 20 December 2019

Pilar García Parejo,[1] Antonio Campos-Jara,[2] Enric García-Caurel,[3] Oriol Arteaga,[3,4] and Alberto Álvarez-Herrero[2,a)]

AFFILIATIONS

[1]ISDEFE, Beatriz de Bobadilla 3, 28040 Madrid, Spain
[2]Space Optics Area, Instituto Nacional de Técnica Aeroespacial, INTA, Ctra de Ajalvir km4, 28850 Madrid, Spain
[3]Laboratoire de Physique des Interfaces et des Couches Minces (LPICM), CNRS, Ecole Polytechnique, IP Paris, 91128 Palaiseau, France
[4]Dep. Física Aplicada, Feman Group, IN2UB, Universitat de Barcelona, 08028 Barcelona, Catalonia, Spain

Note: This paper is part of the Conference Collection: 8th International Conference on Spectroscopic Ellipsometry 2019, ICSE.
[a)]**Electronic mail:** alvareza@inta.es

ABSTRACT

Liquid crystal variable retarders (LCVRs) will be used for the first time in a space instrument, the Solar Orbiter mission of the European Space Agency, as polarization states analyzers (PSAs). These devices will determine the Stokes parameters of the light coming from the Sun by temporal polarization modulation, using the so-called modulation matrix **O**. This is a matrix constituted by the first rows of properly selected PSA Mueller matrices. Calibrating a space instrument, in particular, finding **O**, is a critical point because in a spacecraft there is no possibility of physical access. Due to the huge difficulty in calibrating the complete instruments in all possible scenarios, a more complete calibration of the individual components has been done in ground in order to make extrapolations to obtain **O** in-flight. Nevertheless, apart from the individual calibrations, the experimental errors and nonideal effects that inhibit the system to reach the designed and theoretical values must be known. In this work, description and study of these effects have been done, focusing on the nonideal effects of the LCVRs and the azimuthal misalignments between the optical components of the PSA during the mechanical assembly. The Mueller matrix of a representative LCVR has been measured and mathematically decomposed by logarithm decomposition, looking for values of circular birefringence and fast axis angle variations as a function of voltage. These effects, in the absence of other nonidealities, affect the polarimetric performance, reducing the polarimetric efficiencies in some cases until 11%. Nevertheless, in this case, they are negligible if compared to the other nonideality studied, which are the azimuthal misalignments between the PSA optical components. The study presented in this work is key to extrapolate the PSA **O** matrix if the expected instrumental set-point temperatures are not reached in flight and can be used for the design and implementation of other polarimetric instruments.

I. INTRODUCTION

Liquid crystal variable retarders (LCVRs) will be used for the first time in a space instrument, the Solar Orbiter mission of the European Space Agency. In this mission, they will be part of the polarization states analyzers (PSAs)[1] of two of the ten scientific instruments: Polarimetric and helioseismic imager (PHI[2]) and multielement telescope for imaging and spectroscopy (METIS[3]). Both instruments are Stokes polarimeters, optical instruments that determine the Stokes parameters of the incoming light using polarization optic elements: wave-retarders (LCVRs) and polarizers. The determination of the four Stokes parameters of incoming light is carried out by modulating the signal, using the so-called modulation matrix **O**.[4] This is a system of linear equations formed by the first rows of properly selected PSA Mueller matrices. Modulation matrix and,

therefore, PSA Mueller matrices are key to the polarimetric instruments and must be properly known and calibrated. Nevertheless, calibrating the instrument, in particular, the modulation matrix in a space mission is a critical point because in a spacecraft there is no possibility of physical access. Therefore, calibration must be done in ground and, if possible, in-flight calibration should be also implemented. The modulation matrices of the complete instruments were calibrated in-ground at the expected set-point temperatures, but deviations from these expected scenarios can occur during the mission lifetime. Due to the huge difficulty in calibrating the complete instruments at all possible scenarios, a more complete calibration of the individual components was done. The objective is to determine, through the individual calibrations, the modulation matrix at different conditions during the mission. For this purpose, the optical retardance response of all flight LCVRs were thoroughly and individually measured in a large operating temperature range by generalized ellipsometry. Nevertheless, the final effective LCVR optical retardances in the PSA assembled could be different from those determined during the individual calibration because of experimental discrepancies. In addition, other nonidealities and experimental errors must be considered: a nonideal optical response of the LCVRs (circular birefringence, depolarization, and circular or linear dichroism) and tilt and azimuthal misalignments of the polarizing elements (LCVRs and polarizers). All these effects contribute to a different extent to the complete Mueller matrix and, therefore, the modulation matrix, and they cannot be neglected. For this reason, the Mueller matrices of a representative LCVR cell in a temperature range of 30–80 °C and a wavelength range of 450–1000 nm were measured in a complete Mueller matrix polarimeter and analyzed.

In this work, the measurements of the LCVR Mueller matrices, the analysis of all nonideal effects, and its impact on their performance as polarization modulators are presented. This analysis will provide valuable information to infer the modulation matrix of the Solar Orbiter polarimeters at all space mission possible scenarios. Moreover, the description and analysis of the nonideal effects affecting the LCVRs will allow the design and implementation of other polarimetric instruments on-ground and on-board future space missions.

II. THEORY

A. Modulation matrix O

Stokes polarimeters, or PSA, are devices that determine the Stokes parameters of the light coming from an object (I, Q, U, and V). They work modulating the incoming polarization state of light by using polarization optics as waveplates (e.g., LCVRs) and polarizers defined through Mueller matrices. Nevertheless, as common photodetectors are only sensitive to the intensity of light (I), but insensitive to the rest of the Stokes parameters (Q, U, and V), we are only sensitive to the first row of the PSA Mueller matrix. As we need to measure four quantities, we need to change the PSA Mueller matrix at least four times to have four measurements of the output light intensity (I_o). These changes in the PSA Mueller matrix are accomplished by the application of electric fields to the LCVRs, which produce different optical retardances. A linear equation system constituted by four different first rows of PSA Mueller matrices is obtained, which is known as the modulation matrix $\mathbf{O}$,

$$\begin{pmatrix} I_o^{(1)} \\ I_o^{(2)} \\ I_o^{(3)} \\ I_o^{(4)} \end{pmatrix} = \begin{pmatrix} M_{11}^{(1)} & M_{12}^{(1)} & M_{13}^{(1)} & M_{14}^{(1)} \\ M_{11}^{(2)} & M_{12}^{(2)} & M_{13}^{(2)} & M_{14}^{(2)} \\ M_{11}^{(3)} & M_{12}^{(3)} & M_{13}^{(3)} & M_{14}^{(3)} \\ M_{11}^{(4)} & M_{12}^{(4)} & M_{13}^{(4)} & M_{14}^{(4)} \end{pmatrix} \begin{pmatrix} I \\ Q \\ U \\ V \end{pmatrix} = \mathbf{OS}. \quad (1)$$

The inverse of the modulation matrix is the demodulation matrix $\mathbf{D}$, which allows determining the incoming light Stokes vector ($\mathbf{S}$) from the intensity measurement vector ($\mathbf{I_o}$),

$$\mathbf{S} = \mathbf{D}\mathbf{I_o}. \quad (2)$$

The PSA changes must provide sufficiently different configurations to be able to have well-conditioned $\mathbf{O}$ and $\mathbf{D}$ matrices in order to be invertible. This is quantified by the $\mathbf{D}$ condition number[5] or the efficiency vector.[4] The efficiency vector gives a measure of the error propagation level for each one of the Stokes vector components, given by

$$\boldsymbol{\varepsilon_i} = \left(n \sum_{j=1}^{n} D_{ij}^2\right)^{-1/2}, \quad (3)$$

where n is the number of measurements and i goes from 1 to 4, and ε_1, ε_2, ε_3, and ε_4 are the efficiency vectors for I, Q, U, and V Stokes parameters, respectively. Maximizing the efficiency vector for a specific Stokes component maximizes the signal-to-noise ratio for that specific component and, therefore, the sensitivity to determine it. Theoretical considerations show that the maximum obtainable polarimetric efficiencies for a complete polarization modulator system where homogeneous polarimetric efficiencies are required are

$$\boldsymbol{\varepsilon_i} = \begin{pmatrix} 1 & 1/\sqrt{3} & 1/\sqrt{3} & 1/\sqrt{3} \end{pmatrix} = \begin{pmatrix} 1 & 0.577 & 0.577 & 0.577 \end{pmatrix}. \quad (4)$$

1. Optimum configuration

A PSA typical configuration is shown in Fig. 1. This PSA configuration,[1] used in the PHI instrument, consists of two antiparallel nematic LCVRs with their fast axes aligned at 45° with respect to each other, followed by a linear polarizer at 0° with respect to the fast axis of the first LCVR. With this PSA configuration, a representative set of LCVR optical retardances theoretically give optimum modulation matrices, and therefore, maximum polarimetric efficiencies are shown in Fig. 2. These optical retardance values are used in SO/PHI instrument.

The need to use specific values of the LCVR optical retardances makes mandatory the individual calibration of the LCVRs, i.e., the optical retardance versus voltage at the PSA set-point working temperatures. Nevertheless, LCVRs' individual calibrations do not assure an optimum modulation matrix of the ensemble. In real systems, nonidealities and experimental variations (Sec. III B) occur resulting in a deviation from the theoretical ideal system specified in Fig. 2. For this reason, we always need to calibrate $\mathbf{O}$. In polarimetric instruments in-ground, where physical access is possible, $\mathbf{O}$ can be easily calibrated and recalibrated. If $\mathbf{O}$ measured during calibration is far from the optimum, then a fine-tuning[6] of

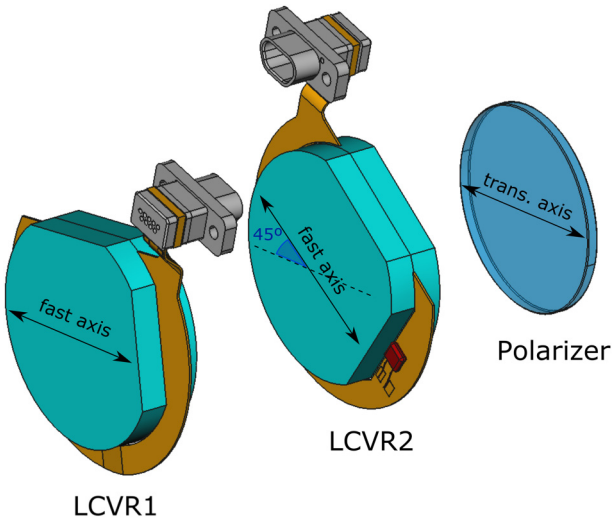

FIG. 1. PSA configuration.

LCVRs' driving voltages is carried out in order to obtain a modulation matrix as close as possible to the optimum.

Nevertheless, in a space instrument, such as PHI and METIS, recalibration is limited because physical access is not possible. Then, calibration must be carried out in-ground as through as possible taking into account all possible scenarios during the mission lifetime. As said previously, calibrating complete instruments at all possible scenarios is not feasible; but from the available in-ground calibrations, it is possible to make extrapolations. Calibrations in-ground performed for PHI instrument are described in Sec. III A.

III. RESULTS AND DISCUSSION

A. Calibrations in-ground for SO/PHI instrument

The individual calibration of LCVRs was carried out using generally ellipsometry in a variable angle spectroscopic ellipsometer (VASE) from J. A. Woolam Co., Inc. This calibration consisted of the measurement of each LCVR retardance versus voltage curve at eight temperatures between 30 and 80 °C at the operative PHI wavelength (617.3 nm). This calibration is performed using a spot beam reaching a small area in the center of the sample.

After the mechanical assembly of the flight LCVRs in the PSA, the calibration of the **O** matrix is carried out in an experimental setup consisting of a polarization states generator (PSG) and an intensity system detection. Seventy-three different known polarization states are introduced using the PSG, which consisted of a polarizer followed by a quarter waveplate at different azimuthal angles. Through inversion of matrix **S**, constituted for different Stokes parameters introduced, in Eq. (1), the matrix **O** is obtained. Note that the optical setup is arranged to take images; thus, the determination of **O** is performed pixel by pixel, i.e., each pixel in the image has a calculated modulation matrix **O**. As good homogeneity is observed, which involves good LCVRs' homogeneity, matrix **O** shown in this work is an average of all the pixels of the image. This calibration was done at a set-point of 40 °C. Finally, the PSA was assembled in the complete PHI instrument, and calibrations of **O** using the similar setup were performed at 40 and 50 °C. Once the individual PSA is assembled in the PHI instrument, nonidealities of the complete optical system such as instrumental residual polarization of the instrument will be introduced in the final matrix **O**. Both calibrations, the individual PSA and the PSA assembled in the PHI instrument, are fine-tuned in order to have the modulation matrix as close as possible to the optimum and maximize the polarimetric efficiencies. The fine-tuned modulation matrix will be used to extract incoming Stokes parameters if during the mission the expected set-point temperatures are reached. However, if there are deviations from the expected scenarios, we would need to infer **O**. For inferring **O**, apart from the calibrations of the respective optical components, the experimental errors and nonidealities that could affect the system in its different steps must be well-known. These effects and their contribution to **O** are described in Sec. III B.

B. Experimental errors and nonideal effects

A scheme of experimental errors and nonideal effects that affect a polarimetric instrument in its different calibration and assembly steps is shown in Fig. 3.

An important experimental error is due to the differences between the real retardance produced in the LCVRs with respect to the optimal ones specified in Fig. 2. The origins of such discrepancies can be multiple. For instance, temperature discrepancies between the temperature control setup in the LCVR individual calibration and the complete PSA calibration, or

Optimal optical retardances (deg)	Optimal modulation matrix	Maximum polarimetric efficiencies
LCVR1 (δ=225, 225, 315, 315) LCVR2 (δ=234.74, 125.26, 54.74, 305.26)	$O=\begin{pmatrix} 1 & -0.577 & 0.577 & -0.577 \\ 1 & -0.577 & -0.577 & 0.577 \\ 1 & 0.577 & -0.577 & -0.577 \\ 1 & 0.577 & 0.577 & 0.577 \end{pmatrix}$	$\begin{matrix} I & Q & U & V \end{matrix}$ $\varepsilon = (1 \;\; 0.577 \;\; 0.577 \;\; 0.577)$

FIG. 2. Optimum modulation scheme configuration.

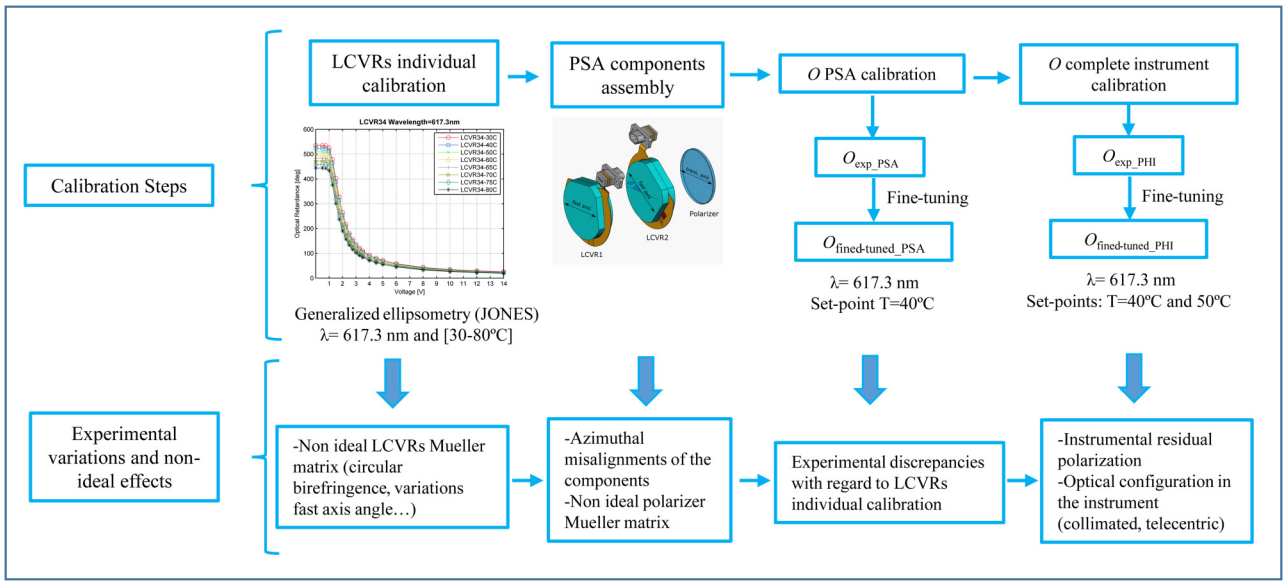

FIG. 3. Scheme of the experimental errors and nonidealities found during the calibration steps.

thermal gradients along the LCVR clear aperture could produce different optical retardances than expected.[7] LCVR voltage sensitivity[8] must be evaluated taking into account the voltage resolution of the used driving equipment. Other effects are retardance inhomogeneity along the LCVR clear aperture, dependence on the angle of incidence (AOI) along the field of view of the optical instrument,[9] and chromatism.[10] Additionally, the final optical configuration of the PSA in the instrument will play an important role. In collimated configuration, as in the METIS instrument, the light beams reach the PSA with different AOIs that produce a diversity of LCVR optical retardances. In a telecentric configuration, as in PHI instrument, the cones of light corresponding to different fields going through the LCVRs will produce a depolarization effect.

Other optical components can also be sources for nonidealities: the polarizer could have nonideal diattenuation; lenses and mirrors of the complete optical instrument can introduce residual polarization. In addition, besides linear birefringence, LCVRs could exhibit other effects that are contained in their Mueller matrix, such as dichroism, circular birefringence, depolarization, etc. Finally, azimuthal misalignments between the PSA polarization components could occur during the mechanical assembly.

All these effects are included in the modulation matrix measured of the complete instrument ($\mathbf{O}_{\text{exp\_PHI}}$) at set points 40 and 50 °C and mostly compensated by fine-tuning ($\mathbf{O}_{\text{fined-tuned\_PHI}}$). Nevertheless, if these temperatures cannot be reached in-flight, for the determination of $\mathbf{O}$, all these effects must be taken into account. In this work, we focus on the nonideal effects of the LCVR Mueller matrix and the possible misalignments during the mechanical assembly of the PSA optical elements that are described and studied in Secs. III B 1 and III B 2.

1. LCVRs' nonideal Mueller matrix

The ideal Mueller matrix for an optical retarder with fast axis aligned with x and retardance δ is expressed as

$$\mathbf{M} = \begin{pmatrix} 1 & 0 & 0 & 0 \\ 0 & 1 & 0 & 0 \\ 0 & 0 & \cos\delta & -\sin\delta \\ 0 & 0 & \sin\delta & \cos\delta \end{pmatrix}. \tag{5}$$

This ideal optical retarder Mueller matrix only considers linear retardance. Nevertheless, these devices could present other nonideal properties that would be contained in the Mueller matrix elements. For this reason, the complete Mueller matrix of an LCVR belonging to same batch than flight LCVRs has been measured using a spectroscopic Mueller polarimeter (Smart SE from HORIBA Scientific) in LPICM facilities. Smart SE provides normalized full Mueller matrices of the probed sample in a continuous spectral range from 450 to 1000 nm with a resolution of 3 nm. The measurements have been done as a function of voltage in a temperature range of 30–80 °C in transmission configuration. As a representative example, the Mueller matrices measured for 40 °C and operative PHI wavelength (617.3 nm) are shown in Fig. 4. These matrices have been rotated with regard to its fast axis position to be aligned with x. Additionally, they have been compared with the ideal Mueller matrix generated by using Eq. (5) and the optical retardance values of the same LCVR obtained from its individual calibration (generalized ellipsometry). Elements that in ideal conditions should be equal to either zero or one; in real measurements, they show different values that need to be taken into account. In fact, noticeable differences are found for the elements M_{23}, M_{24}, M_{32}, and M_{42}.

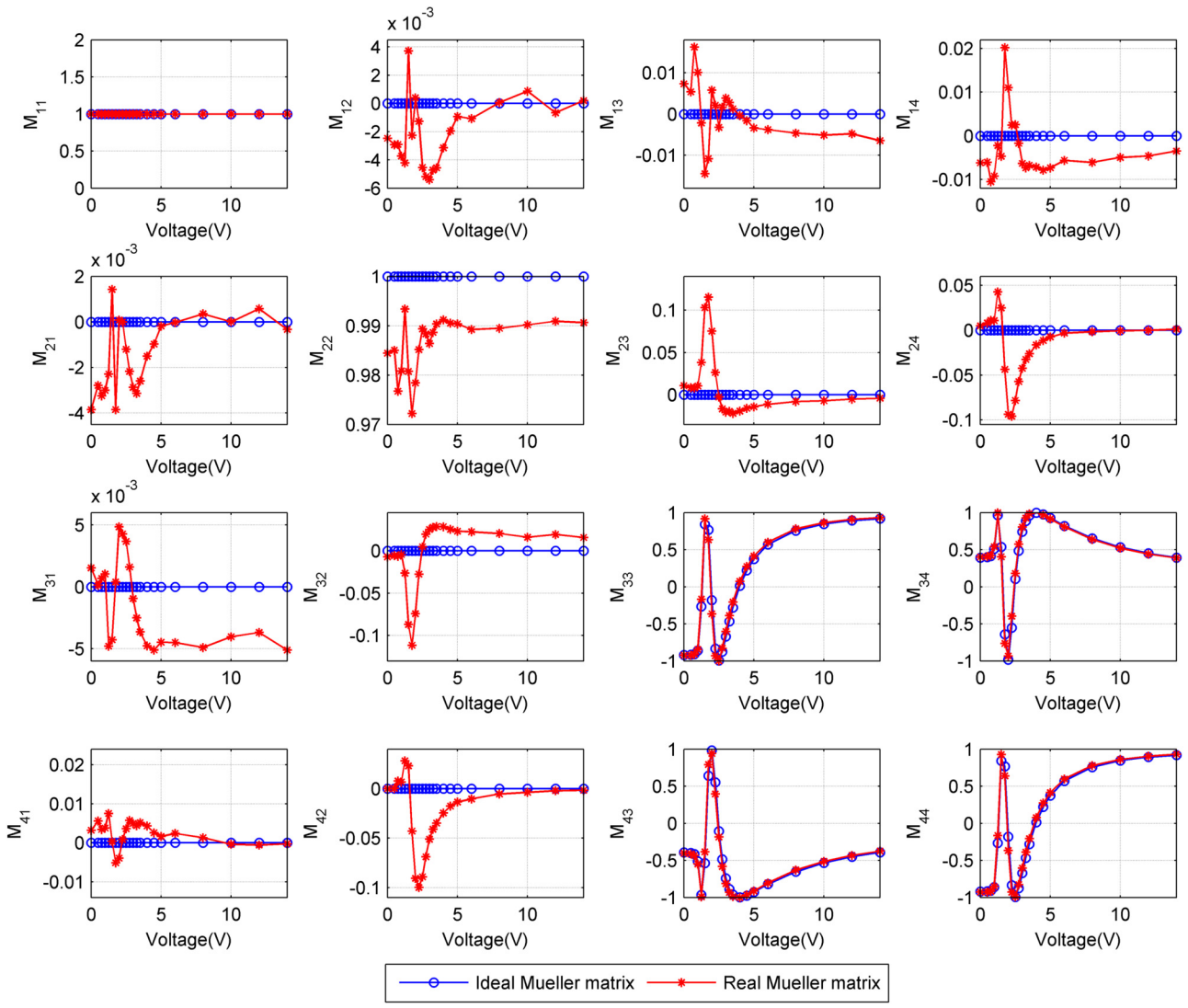

FIG. 4. Comparison between ideal and real LCVR Mueller matrices measured in a HORIBA Mueller ellipsometer as a function of voltage.

Logarithm decomposition[11,12] has been applied to the Mueller matrices measured to extract the basic polarimetric properties, i.e., linear dichroism, circular dichroism, fast axis angle, linear birefringence, circular birefringence, and depolarization as shown in Fig. 5. Low linear and circular dichroism is observed. This could be attributed to the Fresnel reflection/transmission effect at the LCVR multiple internal surfaces that shows a dependence on the driving voltage due to different LC director orientations that cause changes to the effective refractive index. The other effect observed is an LC fast axis orientation dependence on driving voltage, one that is in accordance with that observed by other researchers.[13,14] A non-negligible presence of circular birefringence can also be expected if there are small misalignments between substrates. Nevertheless, measuring a small circular birefringence in the presence of much larger linear birefringence effects is a difficult problem, and in fact, it has frustrated researchers for decades, with the most representative example being the measurement of the circular birefringence of quartz in directions different than the optic axis.[15] Mueller matrix polarimetry is a suitable technique for this analysis because it allows separating linear from circular birefringence. Nevertheless, still great care is needed in the data analysis because one needs to take into account the changes in the order of birefringence to physically obtain representative values.[15–17] These effects are currently being studied in detail, taking into account the spectral evolution of the Mueller matrices at each voltage and temperature, and will be presented in a future work. On the other hand, the change of sign

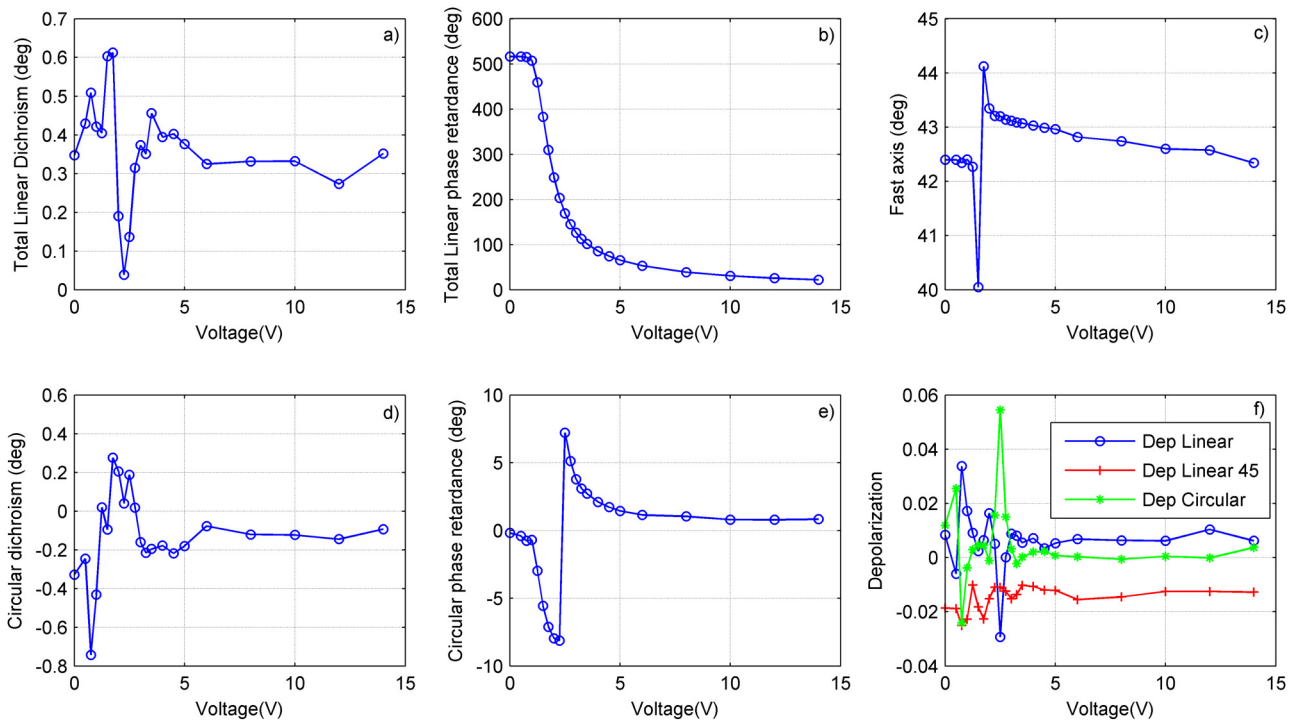

FIG. 5. LCVR polarimetric properties as a function of voltage at 40 °C and $\lambda = 617.3$ nm obtained from logarithm decomposition. (a) Total linear dichroism, (b) total linear phase retardance, (c) LC fast axis, (d) circular dichroism, (e) circular phase retardance, and (f) depolarization.

of the circular birefringence is produced when the LCVR behaves as a halfwave plate (180° of linear and circular phase retardation) and the birefringence changes order. These effects are currently being studied and will be presented in a future work.

Another valuable piece of information from the logarithm decomposition in Fig. 5 is the depolarization degree, which, in the present case, is negligible. As the LCVR does not show any depolarization, we can use the Jones–Mueller transformation,[18] which is defined as

$$\mathbf{M} = \mathbf{A}\langle \mathbf{J} \otimes \mathbf{J}^{*} \rangle \mathbf{A}^{-1}, \tag{6}$$

where $\mathbf{M}$ is the Mueller matrix, $\mathbf{J}$ is the Jones matrix, $\otimes$ denotes the Kronecker product of matrices, and $\mathbf{A}$ is

$$\mathbf{A} = \begin{pmatrix} 1 & 0 & 0 & 1 \\ 1 & 0 & 0 & -1 \\ 0 & 1 & 1 & 0 \\ 0 & i & -i & 0 \end{pmatrix}.$$

This transformation allows us to derive the complete Mueller matrices from Jones measurements of the LCVR individual calibration. We have performed this transformation to the Jones matrices of the representative LCVR measured in the VASE ellipsometer, and we have compared them to the Mueller matrices measured in the Mueller polarimeter. The comparison is shown in Fig. 6. Both Mueller matrices are very similar considering that they were taken by different instruments, and some experimental discrepancies could have occurred. These results confirm that it is possible to systematically apply the Jones–Mueller transformation to the ensemble of Jones measurements of the LCVRs' individual calibration of the flight PHI LCVRs taken with the VASE spectroscopic ellipsometer. On one hand, this will allow us to determine, as a general case, the contribution of these nonideal effects in PSAs' modulation matrices constituted of LCVRs. On the other hand, we can determine the contribution of these effects in our case, in PHI PSA.

We have applied the Jones–Mueller transformation to the calibration of in-ground individual flight cells LCVR_1 and LCVR_2 of PHI PSA. Then, we have evaluated the corresponding Jones–Mueller matrices that would be obtained when these optical elements are operated according to the PHI modulation scheme (Fig. 2), considering ideal azimuthal positions of the optical elements (Fig. 1). Then, from these matrices, the corresponding $\mathbf{O}$ matrices, labeled as $\mathbf{O}_{\mathrm{nonideal}}$, are shown and compared to the ideal ($\mathbf{O}_{\mathrm{ideal}}$) in Table I.

Changes in the modulation matrices occur with regard to the ideal when nonideal effects of LCVRs are included. Additionally, these changes reduce the polarimetric efficiencies for ε_1, ε_2, ε_3, and ε_4 to 0.994 (0.5%), 0.543 (6%), 0.546 (5.4%), and 0.511 (11%), respectively. Note that the specifications of polarimetric efficiencies

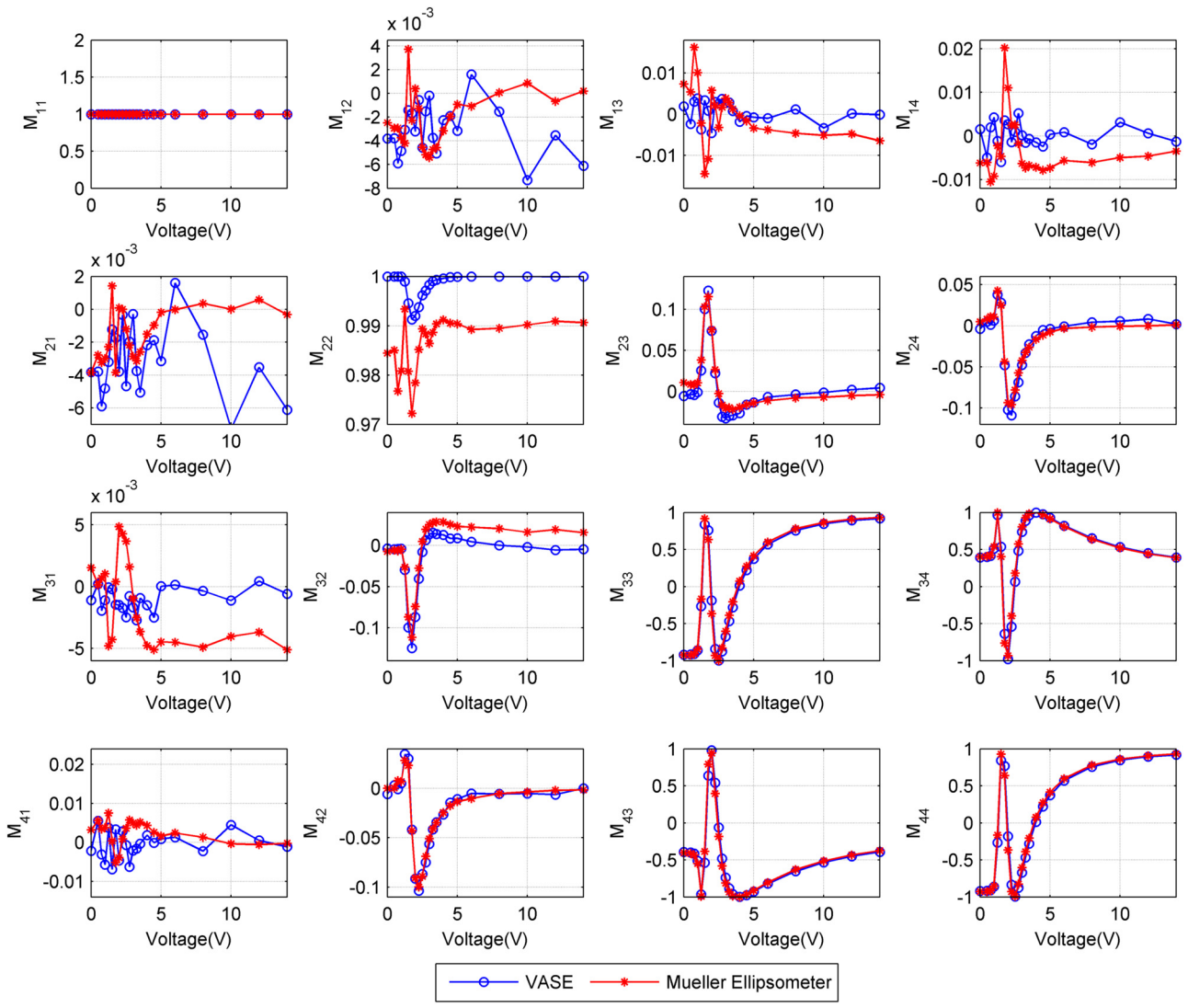

FIG. 6. Comparison between LCVR Jones–Mueller matrix obtained from VASE measurements and LCVR Mueller matrix measured in a HORIBA Mueller ellipsometer at 40 °C and $\lambda = 617.3$ nm.

for PHI PSA to comply with Solar Orbiter scientific requirements are $\varepsilon \geq$ (1 0.5 0.5 0.5). Therefore, these effects are not negligible particularly for ε_4, where a reduction of 11% is found. In the absence of other nonidealities, the LCVRs' nonideal effects contained in their Mueller matrix cannot be neglected.

We have compared the PSA **O** matrix calculated using the nonideal Mueller matrices ($\mathbf{O}_{\text{nonideal}}$) with $\mathbf{O}_{\text{exp\_PSA}}$, the PSA **O** matrix measured experimentally during the calibration in-ground before the fine-tuning process (Fig. 3). This has been done in order to verify whether the LCVRs' nonideal response could explain the nonideal modulation matrix measured experimentally (see Table I). It can be seen that the values do not fully agree. The difference between these two modulation matrices can be evaluated using the root mean square error (RMSE) as a figure of merit,[6] which is defined as

$$\text{RMSE} = \sqrt{\frac{\sum_{ij}\left[(O_A)_{ij} - (O_B)_{ij}\right]^2}{4\,x\,n}}, \tag{7}$$

where O_A and O_B are two different modulation matrices and n is the number of modulation states, which is 4 for our PSA. The RMSE between $\mathbf{O}_{\text{nonideal}}$ and $\mathbf{O}_{\text{exp\_PSA}}$ is 0.1516. Based on these results, the nonideal optical response of the individual LCVRs cannot fully explain by itself the discrepancies between the ideal and the final

TABLE I. Minimization results showing the resulting **O** matrices after fitting the azimuthal orientation of the individual LCVRs. Two cases are illustrated. First and second minimizations correspond to cases when $\mathbf{O}_{ideal}$ and $\mathbf{O}_{nonideal}$ are taken as starting points in the minimization routine, respectively.

Case	Optical parameters	Modulation matrices	Modulation efficiencies
O calculated using ideal Mueller matrices	$LCVR_1(\delta = 225, 225, 315, 315)$ $LCVR_2$ ($\delta = 234.74, 125.26, 54.74, 305.26$) $LCVR_1$ Azimuth: 0° $LCVR_2$ Azimuth: 45° Polarizer Azimuth: 0°	$O_{ideal} = \begin{pmatrix} 1.000 & -0.577 & 0.577 & -0.577 \\ 1.000 & -0.577 & -0.577 & 0.577 \\ 1.000 & 0.577 & -0.577 & -0.577 \\ 1.000 & 0.577 & 0.577 & 0.577 \end{pmatrix}$	$\varepsilon = (1.000 \quad 0.577 \quad 0.577 \quad 0.577)$
O calculated using nonideal Mueller matrices	$LCVR_1(\delta = 225, 225, 315, 315)$ $LCVR_2$ ($\delta = 234.74, 125.26, 54.74, 305.26$) $LCVR_1$ Azimuth: 0° $LCVR_2$ Azimuth: 45° Polarizer Azimuth: 0°	$O_{nonideal} = \begin{pmatrix} 1.003 & -0.557 & 0.409 & -0.545 \\ 1.002 & -0.558 & -0.519 & 0.560 \\ 0.999 & 0.587 & -0.541 & -0.590 \\ 1.000 & 0.500 & 0.688 & 0.358 \end{pmatrix}$	$\varepsilon = (0.994 \quad 0.543 \quad 0.546 \quad 0.511)$
O experimentally measured during PSA calibration in-ground before fine-tuning	LCVR1 ($\delta = 225, 225, 315, 315$) LCVR2 ($\delta = 234.74, 125.26, 54.74, 305.26$)	$O_{exp\_PSA} = \begin{pmatrix} 0.997 & -0.661 & 0.554 & -0.460 \\ 0.997 & -0.442 & -0.329 & 0.800 \\ 1.012 & 0.590 & -0.711 & -0.242 \\ 0.993 & 0.345 & 0.681 & 0.576 \end{pmatrix}$	$\varepsilon = (0.950 \quad 0.494 \quad 0.555 \quad 0.531)$

modulation matrices measured, and therefore, other nonideal effects must be considered. In Sec. III B 2, the effect of the misalignment of the azimuthal orientation of the axis of the LCVRs will be discussed.

2. Azimuthal misalignments

The optical elements of METIS and SO/PHI PSAs are placed in mechanical mounts in fixed positions in the mechanical structure of the instruments. The final azimuthal positions of these elements will depend on the manufacturing tolerances of the optical elements and the mechanical assembly. This could result in azimuthal angles between the polarizing elements (LCVRs and polarizers) different from the designed values depicted in Fig. 1.

To evaluate the contribution of the azimuthal misalignments in the nonideal modulation matrix measured, we have used a minimization of the RMSE function in Eq. (7), where $\mathbf{O}_A$ is a starting modulation matrix and $\mathbf{O}_B$ is the experimental PSA **O** measured ($\mathbf{O}_{exp\_PSA}$) during the calibration in-ground. The minimization parameters are the azimuthal positions of the optical elements ($LCVR_1$, $LCVR_2$, and the polarizer). Two minimizations have been done. The first minimization was carried out by using the matrix $\mathbf{O}_{ideal}$ as the starting modulation. The second minimization was carried out by using the modulation matrix calculated as the starting modulation taking into account the nonidealities of the LCVRs Mueller matrices ($\mathbf{O}_{nonideal}$). As we use the polarizer azimuth as our polarization reference system and we are only interested in determining the relative azimuths between the optical elements, its position will be fixed in the minimization at 0°. The results of the minimization are shown in Table II.

We observe that for both cases introducing variable azimuths in the minimization reduces drastically the values of RMSE (0.0992 and 0.0799, respectively) to be compared to an RMSE of 0.1516 discussed in Sec. III B 1. Therefore, in view of these results, it can be said that the mechanical misalignment is the principal cause of discrepancy between the ideal and the real optical response of the PSA, whereas the nonideal effect of the LCVRs, not being negligible, plays a second role. The misalignment effect explains an RMSE reduction from 0.1516 to 0.0992 (73% of total reduction), while the nonidealities account for a reduction from 0.0992 to 0.0799 (27% of total reduction). Additionally, we observe that the misalignment error between LCVR cells is relatively small (2°): the minimization provides an angle between LCVRs equal to 47°, to be compared to

TABLE II. Minimization results showing the resulting **O** matrices after fitting the azimuthal orientation of the individual LCVRs. Two cases are illustrated. First and second minimizations correspond to cases when $\mathbf{O}_{ideal}$ and $\mathbf{O}_{nonideal}$ are taken as starting points in the minimization routine, respectively.

Case	Elements azimuths fitted	**O** fitted	RMSE
First minimization Starting matrix: $\mathbf{O}_{ideal}$	Minimization: LCVR1: 5.5° (fitted) LCVR2: 52.0° (fitted) Polarizer: 0° (fixed) Angle between LCVR cells: 46.5°	$0 = \begin{pmatrix} 1.000 & -0.680 & 0.633 & -0.369 \\ 1.000 & -0.466 & -0.467 & 0.751 \\ 1.000 & 0.697 & -0.588 & -0.412 \\ 1.000 & 0.483 & 0.512 & 0.710 \end{pmatrix}$	RMSE = 0.0992
Second minimization Starting matrix: $\mathbf{O}_{nonideal}$	Minimization: LCVR1: 6.3° (fitted) LCVR2: 53.7° (fitted) Polarizer: 0° (fixed) Angle between LCVR cells: 47.4°	$\begin{pmatrix} 1.001 & -0.616 & 0.521 & -0.338 \\ 1.007 & -0.442 & -0.364 & 0.746 \\ 0.998 & 0.733 & -0.545 & -0.384 \\ 0.999 & 0.426 & 0.620 & 0.537 \end{pmatrix}$	RMSE = 0.0799

45° in the ideal case. A misalignment error of about 2° is within the mechanical tolerances. However, the polarizer misalignment is higher, around 6°. The polarizer is assembled in a mechanical mount aligning its optical axis to eye searching a null using another polarizer, which would explain a higher error.

IV. CONCLUSIONS

The nonideal response of LCVRs and their respective mechanical mounting errors have been discussed as possible causes to explain the observed differences between the expected (ideal) and measured modulation matrices of a PSA build using such LCVRs. The present study has been carried out taking into consideration the special circumstances of a space mission, in particular, the Solar Orbiter mission. The LCVRs' Mueller matrices have been measured, finding nonidealities that contribute in the final modulation matrix of the PSA. In the absence of other nonidealities, it has to be considered that they can reduce polarimetric efficiencies in some cases until 11%. Nevertheless, for our case, they do not explain the experimental modulation matrices measured and they can be considered negligible if compared to the other nonideality studied, the azimuthal misalignments. The results of this work will be used for inferring the PSA **O** matrix in flight for the Solar Orbiter if the expected scenarios of temperature are not reached. Moreover, this valuable information can be used for the design and implementation of other polarimetric instruments, in particular, for future polarimetric instruments in space missions.

ACKNOWLEDGMENTS

The authors are very grateful to all the members of the SO/PHI team and to the INTA team, in particular. This work would not have been possible without them. This project was funded by the Ministerio de Ciencia, Innovación y Universidades (No. ESP2016-77548-C5-4-R).

REFERENCES

[1]A. Álvarez-Herrero *et al.*, Proc. SPIE **9613**, 96130I (2015).
[2]S. K. Solanki *et al.*, "The polarimetric and helioseismic imager on Solar Orbiter," Astron. Astrophys. (to be published).
[3]E. Antonucci *et al.*, "Metis: The Solar Orbiter visible light and ultraviolet coronal imager," Astron. Astrophys. (to be published).
[4]J. C. del Toro Iniesta and M. Collados, Appl. Opt. **39**, 1637 (2000).
[5]J. S. Tyo, Appl. Opt. **41**, 619 (2002).
[6]A. Álvarez-Herrero, P. García Parejo, and M. Silva-López, Opt. Express **26**, 12038 (2018).
[7]P. García Parejo and A. Álvarez-Herrero, Opt. Mater. Express **9**, 2681 (2019).
[8]J. C. del Toro Iniesta and V. Martínez-Pillet, Astrophys. J. Suppl. Ser. **201**, 22 (2012).
[9]P. García Parejo, A. Álvarez-Herrero, G. Capobianco, and S. Fineschi, J. Astron. Telesc. Instrum. Syst. **5**, 034002 (2019).
[10]G. Capobianco *et al.*, Proc. SPIE **10698**, 1069830 (2018).
[11]R. Ossikovski, Opt. Lett. **36**, 2330 (2011).
[12]E. García-Caurel, R. Ossikovski, M. Foldyna, A. Pierangelo, B. Drévillon, and A. De Martino, "Advanced Mueller ellipsometry instrumentation and data analysis," in *Ellipsometry at the Nanoscale*, edited by M. Losurdo and K. Hingerl (Springer, Berlin, 2013).
[13]A. R. Tiwary, S. K. Mathew, A. R. Bayanna, P. Venkatakrishnan, and R. Yadav, Sol. Phys. **292**, 49 (2017).
[14]P. Terrier, J. M. Charbois, and V. Devlaminck, Appl. Opt. **49**, 4278 (2010).
[15]O. Arteaga, A. Canillas, and G. E. Jellison, Jr., Appl. Opt. **48**, 5307 (2009).
[16]V. Devlaminck and R. Ossikovski, Opt. Lett. **39**, 3149 (2014).
[17]E. Kuntman, O. Arteaga, J. Antó, D. Cayuela, and E. Bertran, Opt. Pura Apl. **48**, 309 (2015).
[18]R. M. A. Azzam and N. M. Bashara, *Ellipsometry and Polarized Light* (North Holland, Amsterdam, 1988).